iScience

CellPress
OPEN ACCESS

Article

Alphaherpesvirus-mediated remodeling of the cellular transcriptome results in depletion of m6A-containing transcripts

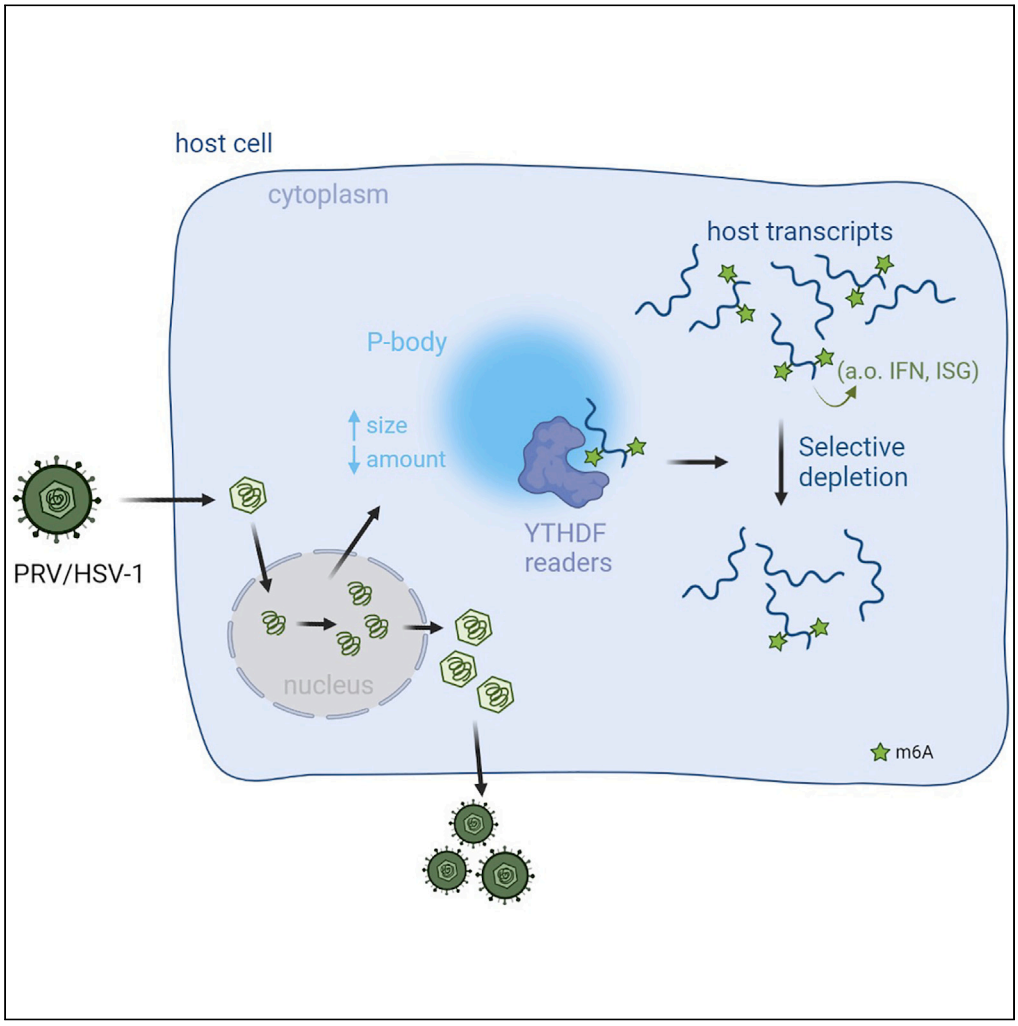

Robert J.J. Jansens, Anthony Olarerin-George, Ruth Verhamme, Aashiq Mirza, Samie Jaffrey, Herman W. Favoreel

herman.favoreel@ugent.be

Highlights

Alphaherpesvirus infection leads to selective depletion of m6A-methylated RNA

This selective depletion depends on the YTHDF family of m6A-binding proteins

YTHDF proteins relocalize to enlarged P-bodies during alphaherpesvirus infection

YTHDF knockdown leads to reduced viral protein and increased ISG expression

Jansens et al., iScience *26*, 107310
August 18, 2023
https://doi.org/10.1016/j.isci.2023.107310

iScience

CellPress
OPEN ACCESS

Article

Alphaherpesvirus-mediated remodeling of the cellular transcriptome results in depletion of m6A-containing transcripts

Robert J.J. Jansens,[1,2,3] Anthony Olarerin-George,[2,3] Ruth Verhamme,[1,3] Aashiq Mirza,[2] Samie Jaffrey,[2,4] and Herman W. Favoreel[1,4,5,*]

SUMMARY

The mechanisms by which viruses regulate host mRNAs during infection are still poorly understood. Several host transcripts that encode proteins that contribute to the anti-viral response contain the N6-methyladenosine nucleotide (m6A). In this study, we investigated if and how viruses from different (sub) families specifically affect m6A-containing host transcripts. Systematic analysis of host transcriptomes after infection with diverse types of viruses showed that m6A-methylated transcripts are selectively downregulated during infection with Sendai virus, African swine fever virus and the alphaherpesviruses herpes simplex virus 1 (HSV-1) and pseudorabies virus (PRV). Focusing on PRV and HSV-1, we found that downregulation of m6A-methylated transcripts depends on the YTHDF family of m6A-binding proteins, and correlates with localization of these proteins to enlarged P-bodies. Knockdown of YTHDF proteins in primary cells reduced PRV protein expression and increased expression of antiviral interferon-stimulated genes, suggesting that virus-induced depletion of host m6A-containing transcripts constitutes an immune evasion strategy.

INTRODUCTION

Viral infection can dramatically change the transcriptome landscape of a host cell. This includes virus modulation of the host transcriptome to redirect host resources to the efficient production of progeny virus, leading to a so-called host-shutoff.[1] This is a non-selective strategy and more specific viral strategies can ensure a preferential downregulation of anti-viral transcripts, leaving transcripts encoding for proteins essential for viral replication relatively untouched. Several studies have attempted to identify and understand factors determining specificity of viral regulation of the host transcriptome.[2–5] However, the specific mechanisms that viruses use to regulate specific host transcripts remain largely unknown.

Over the past years, it has become clear that chemical modifications of mRNA, the so-called epitranscriptome, represent an additional layer of post-transcriptional regulation of gene expression. N6-methyladenosine (m6A) represents the most abundant internal chemical modification in mRNA, and affects several aspects of transcript biology, particularly mRNA degradation.[6] Approximately a quarter of all host transcripts contain at least one m6A site.[7,8] Interestingly, several cellular transcripts that encode immune effectors are highly m6A-methylated.[9–11] Most notably, transcripts encoding antiviral type I interferons (IFN) and several interferon-stimulated genes (ISG), which are expressed as an innate cellular response upon virus infection are highly m6A-modified.[9–12] Different proteins, including cytoplasmic YTHDF proteins, recognize m6A-methylated transcripts, thereby serving as m6A readers that may affect mRNA biology, including nuclear export, transcript degradation, and translation efficiency.[13] Notably, it has been reported that shRNA-mediated depletion of YTHDF reader proteins suppresses viral replication of several viruses from different families, likely through the stabilization of IFN and ISG transcripts.[14–18]

Considering the strong association of m6A with the innate immune response, it would be feasible that viruses specifically affect m6A-methylated transcripts to increase their replication, something that has not been addressed thus far.

[1]Department of Translational Physiology, Infectiology and Public Health

[2]Department of Pharmacology, Weill Medical College, Cornell University, New York NY 10021, USA

[3]These authors contributed equally

[4]Senior author

[5]Lead contact

*Correspondence: herman.favoreel@ugent.be

https://doi.org/10.1016/j.isci.2023.107310

In this study, we systematically compared the effect of infection with viruses from different families on m6A-methylated transcripts or transcripts that lack m6A methylation. We show that while most viruses that were analyzed do not appear to specifically regulate m6A-methylated transcripts, cells infected with Sendai virus, African swine fever virus, and specific alphaherpesviruses, but not beta- or gammaherpesviruses, show a decrease in m6A-methylated transcripts. Destabilization of m6A-methylated transcripts during alphaherpesvirus infection is proportional to the number of m6A sites. The destabilization of m6A-methylated transcripts during alphaherpesvirus infection depends on the YTHDF family of m6A reader proteins and correlates with a localization of the YTHDF proteins to enlarged P-bodies. We show that this process is a post-entry event that does not require the UL41/vhs viral RNAse. Finally, we show that, although YTHDF-mediated destabilization of m6A-containing transcripts is not essential for alphaherpesvirus replication in interferon-deficient cell culture, it instead suppresses the type I interferon response and promotes viral protein production in primary epithelial cells. Overall, these studies suggest a previously uncharacterized mechanism by which specific alphaherpesviruses and other types of viruses control the innate immune response by preferentially inducing degradation of m6A-containing host mRNAs.

RESULTS

Different viruses, including alphaherpesviruses, specifically regulate m6A-methylated transcripts

Gene expression analyses during the replication cycle of several viruses have been previously reported.[19–33] These existing datasets allowed us to determine whether certain viruses globally alter the expression of m6A-containing transcripts during infection. We first analyzed a set of published gene expression datasets of cells infected with different viruses from the NCBI Gene Expression Omnibus (GEO) (Table S1). Differential host gene expression was determined and transcripts were grouped by the number of annotated m6A sites per transcript. The overall pattern of m6A is highly conserved across different cell types and tissues.[6,34,35,36] The high-resolution single-nucleotide resolution maps of m6A that were used in this study, depending on the species in which the gene expression dataset was generated, can be found in Tables S2, S3, and S4. For the analyses of human samples, an m6A map originating from HEK293T cells was used,[36] while the m6A maps originating from two other human cell types (HepG2 and K562) illustrate the strong conservation of m6A methylation patterns over different cell types (Table S2). Next, we calculated a fold change in host gene expression (infection vs. mock) for each transcript. The cumulative distribution of these fold changes was plotted for groups of mRNAs that were binned based on the number of annotated m6A sites.

Analyses of datasets of cells infected with RNA viruses of several different virus families, including *Retroviridae*, *Flaviviridae*, *Coronaviridae*, *Hepeviridae*, and *Orthomyxoviridae* did not show selective regulation proportional to the degree of m6A methylation of host transcripts compared to non-methylated transcripts (Figure 1). Cells infected with DNA viruses from the *Hepadnaviridae* family or the *Poxviridae* family also did not show preferential regulation of m6A-methylated host transcripts. Different members of the *beta-* and *gammaherpesvirinae* subfamilies of the *Herpesviridae* also did not show specific regulation of m6A-methylated host transcripts.

However, infection with members from certain other viruses led to specific regulation of m6A-methylated transcripts. In cells infected with adenovirus, a dsDNA virus, m6A-methylated transcripts were stabilized relative to unmethylated transcripts (Figure 1). Furthermore, cells infected with Sendai virus, a member of the *Paramyxoviridae* family, and African swine fever virus, the sole member of the *Asfarviridae*, showed a preferential downregulation of m6A-containing transcripts (Figure 1). Interestingly, while members of the *beta-* and *gammaherpesvirinae* subfamilies of the *Herpesviridae* family did not show preferential regulation of m6A-methylated transcripts, cells infected with herpes simplex virus 1 (HSV-1), an alphaherpesvirus, showed preferential downregulation of m6A-methylated transcripts proportional to the amount of m6A sites found in the transcript (Figure 1).

To confirm these findings of HSV-1 infected cells, we analyzed all other publicly available RNA-seq datasets of HSV-1 infected cells and also generated an additional RNA-seq dataset of HSV-1 infected HEK293T cells. We found that in all datasets, m6A-containing transcripts were preferentially downregulated compared to unmethylated transcripts (Figure 1). We also analyzed a dataset containing RNA-seq data from the closely related HSV-2 virus.[23] We did not observe the preferential degradation of m6A-methylated transcripts in this HSV-2 dataset (data not shown), but, as will be described in the following text, it is possible that the relatively early time point of infection (8 hpi) of this particular dataset[23] may have been too early to observe

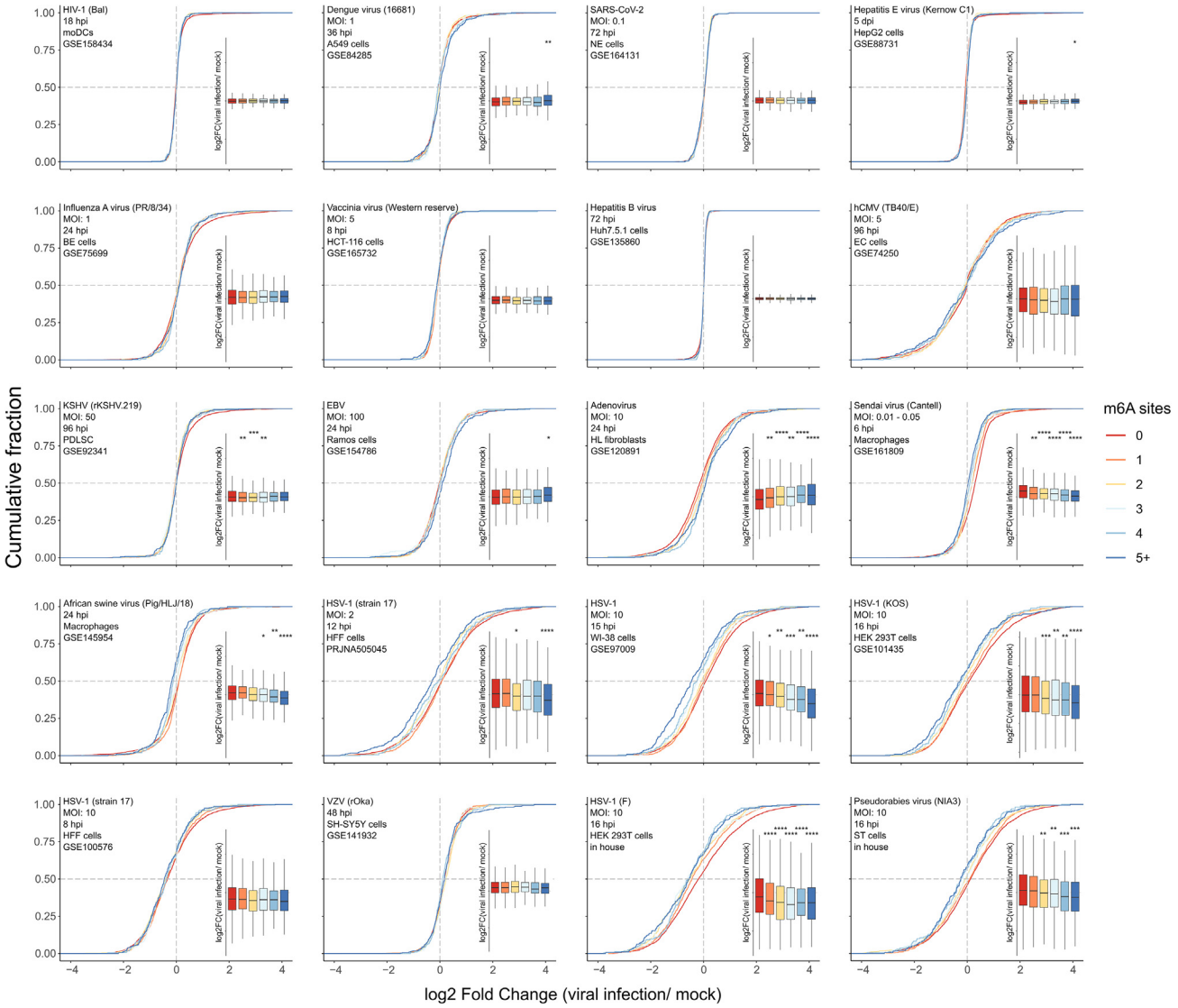

Figure 1. Viruses from different families specifically regulate m6A-containing host cell transcripts

Cumulative distribution plots and bar graphs summarizing gene expression data from different cell lines infected with various viruses, for various durations (hours post infection, hpi), as indicated. When available, specific virus strain and infectious dose (MOI) are indicated. The transcripts expressed in each cell line were binned based on the annotated number of m6A sites per transcript based on previous high-resolution m6A maps (Tables S2, S3, and S4). Transcripts with no m6A sites are shown in red, with 5 or more are dark blue. For most viruses, there was little to no change in gene expression based on the number of m6A sites. However, for several viruses, transcripts that contained m6A showed selectively decreased expression, in proportion to the number of m6A sites. These gene sets show the blue curve to the left of the red curve. In the case of adenovirus, the m6A-containing mRNAs appeared more stable than the non-methylated RNA. Details of the different datasets and the m6A maps used in this analysis can be found in Tables S1, S2, S3, and S4. *$p < 0.05$, **$p < 0.01$, ***$p < 0.001$, ****$p < 0.0001$.

the effect (Figure S3C). An RNA-seq dataset of human neuroblastoma cells infected with another alphaherpesvirus, varicella-zoster virus (VZV),[37] also did not indicate preferential depletion of m6A-containing transcripts (Figure 1). In the latter study, a GFP-expressing variant of the recombinant Oka vaccine strain of VZV was used. This recombinant VZV strain is avirulent due to several mutations in the viral genome acquired during cell culture passage.[38] Hence, it is unclear if infection of cells with a virulent VZV strain may or may not lead to depletion of m6A-containing transcripts.

To further assess whether preferential downregulation of m6A-containing transcripts is conserved in other alphaherpesviruses, we performed RNA-seq assays of porcine ST cells infected with the porcine

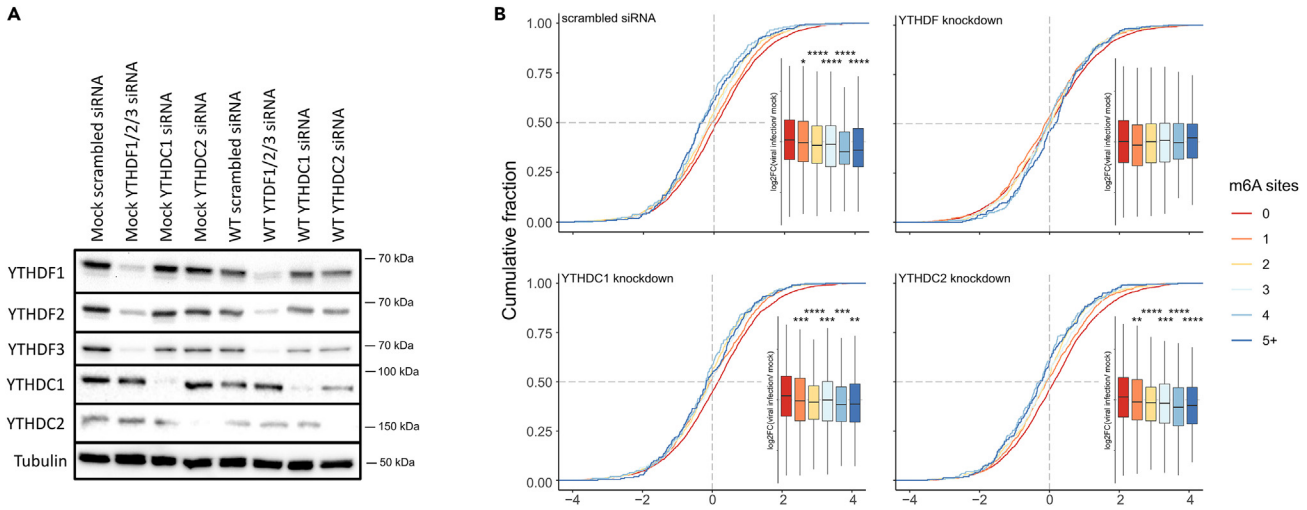

Figure 2. Selective destabilization of m6A-containing transcripts during PRV infection requires the YTHDF proteins

(A) Knockdown efficiency of different siRNAs targeting YTH domain containing proteins determined by western blot. Quantification of western blots indicated that, upon normalization to the tubulin protein control, all YTH-domain containing protein-targeted siRNA treatments reached an efficiency of ≥ 73% target protein reduction (n = 3). PRV-infected cells were inoculated at an MOI of 10 at 48 h after treatment with siRNAs, and analyzed at 16 hpi (n = 2).

(B) Cumulative fold change of transcripts as measured by RNA-seq between mock and PRV-infected ST cells after knockdown of m6A readers alone, or in the case of the YTHDF proteins, in combination (YTHDF1, YTHDF2, and YTHDF3 together). PRV-infected ST cells were inoculated at an MOI of 10 after 48 h treatment with siRNAs and harvested at 16 hpi. Controls were performed using scrambled siRNA. Transcripts were binned based on the number of m6A sites, with the red line representing unmethylated transcripts. Control knockdown, as well as knockdown of YTHDC1 or YTHDC2 did not affect the selective loss of m6A-mRNAs induced by PRV infection. However, the loss of m6A-mRNAs was blocked in cells depleted of YTHDF1, 2, and 3. *p < 0.05, **p < 0.01, ***p < 0.001, ****p < 0.0001.

alphaherpesvirus pseudorabies virus (PRV), and similarly assessed the data for preferential degradation of m6A-containing transcripts. PRV is an alphaherpesvirus of pig that is frequently used as model micro-organism to study general aspects of alphaherpesvirus infection.[39] Notably, PRV-infected cells also displayed a clear reduction in m6A-containing transcripts (Figure 1). Taken together, these data suggest that downregulation of m6A-modified host mRNAs in infected cells appears to be a feature that is conserved in different alphaherpesviruses.

Preferential depletion of m6A-containing transcripts during PRV infection depends on YTHDF m6A reader proteins

Downstream effects of m6A methylation of transcripts are typically mediated by so-called reader proteins. These reader proteins specifically bind to m6A-methylated transcripts and can, among other functions, mark m6A-methylated mRNA for degradation.[40,41] The best characterized group of m6A reader proteins are the YTH-domain containing proteins. Vertebrates encode five YTH-domain containing proteins: three YTHDF homolog, YTHDC1, and YTHDC2.[42] Although the three YTHDF proteins were initially described to have distinct functions, more recent work showed that the YTHDF proteins act redundantly to degrade m6A-containing transcripts.[40,41,43–45]

We therefore asked whether PRV infection-induced downregulation of m6A-containing transcripts is mediated by proteins of the YTH family. To test this, YTHDC1, YTHDC2, or YTHDF1-3, in combination, were knocked down using siRNA. Previous studies have shown that the effect of YTHDF depletion is more prominent when the three YTHDF proteins are knocked down together due to redundancy between these paralogs.[41] In cells knocked down for YTHDC1 or YTHDC2, PRV infection still resulted in a preferential depletion of m6A-containing transcripts that is similar to that observed in scrambled siRNA-treated ST cells (Figure 2). However, the selective depletion of m6A-containing transcripts was abrogated upon knockdown of the YTHDF proteins, indicating that the YTHDF proteins mediate the preferential depletion of m6A-containing transcripts upon PRV infection (Figure 2).

Changes in gene expression upon viral infection can be the result of less RNA being transcribed, or more RNA being degraded. YTHDF proteins are known to cause degradation of m6A-methylated

transcripts,[40,41] indicating that the observed depletion in m6A-containing transcripts observed in PRV-infected cells is caused by degradation of these transcripts. To further confirm this, we used a method called exon-intron split analysis (EISA), a computational method that allows the differentiation of transcriptional and post-transcriptional effects on transcript levels based on the ratio of intronic and exonic reads.[46] Intronic reads are only present in unprocessed pre-mRNA and changes in the amount of intronic reads can thus be used as a measure of transcription. EISA results in a measure for changes in transcription rate (Δintron) and a measure for changes in transcript stability (Δexon-Δintron) for each transcript.[46] We applied this analysis to RNA-seq data from ST cells infected with wild type PRV, both in scrambled siRNA treated cells and in cells in which all three YTHDF proteins were knocked down. While in the dataset of PRV-infected scrambled siRNA treated cells, there was no difference in transcription rates (Δintron) between m6A-methylated and unmethylated transcripts, transcript stability (Δexon-Δintron) was reduced in m6A-containing transcripts, compared to unmethylated transcripts (Figure S1). This further supports the notion that the reduced m6A-mRNA abundance after PRV infection is due to a decrease in their stability.

Further in line with this, the observed difference in transcript stability between m6A-methylated and unmethylated transcripts using EISA was lost in the transcriptomics dataset of PRV-infected YTHDF triple knockdown cells (Figure S1). Together, these results indicate that the decrease in m6A-mRNA stability upon PRV infection is mediated by YTHDF proteins, in line with the previously established functions of these m6A reader proteins.[41,42]

YTHDF readers localize to a reduced number of enlarged P-bodies during PRV or HSV-1 infection

To test whether the YTHDF-dependent destabilization of m6A-methylated transcripts may correlate with an altered expression or an altered localization of the YTHDF proteins during infection, western blot and immunofluorescence assays were performed on virus-infected cells. Western blot showed that none of the three YTHDF proteins was upregulated upon PRV infection, and neither was CNOT1, a central component of the CCR4-NOT complex that executes YTHDF-driven mRNA degradation (Figure 3A). Subsequently, immunofluorescence assays were performed to assess the subcellular localization of YTHDF proteins in mock- or PRV-infected cells. All three YTHDF proteins are normally found in the cytoplasm and show partial co-localization with P-bodies in control cells.[47] We were unable to image YTHDF2 as none of the antibodies that target human and mouse YTHDF2 proteins could detect porcine YTHDF2 in immunofluorescence assays. In mock-infected cells, YTHDF3 showed a rather homogeneous distribution in the cytoplasm with some punctae that co-localize with EDC4, a P-body marker (Figures 3B–3D). YTHDF1 showed a similar redistribution, although a larger amount of YTHDF1 appeared to already localize to P-bodies in mock-infected cells (Figure S2A). Upon infection with PRV, the YTHDF proteins showed obvious and increased co-localization with the P-body marker EDC4 (Figures 3D, S2A, and S2B). Such increased co-localization with P-bodies was also observed in HSV-1-infected HeLa cells (Figure S2C).

Remarkably, fewer and larger puncta of P-bodies could be observed in PRV-infected cells (Figures 3B–3D). Indeed, in mock-infected cells, there were on average 23 $\pm$ 3 EDC4 punctae per cell with an average area of 0.57 $\pm$ 0.06 μm^2, while the number of punctae decreased to 7 $\pm$ 1 per cell ($p = 0.007$) with an increased area of 1.17 $\pm$ 0.08 μm^2 in PRV-infected cells ($p = 0.004$). To determine how P-body number and size change over time as a result of viral infection, we performed a time course experiment of ST cells infected with PRV. The changes in size and number of P-bodies were detectable from 4 to 6 hpi onwards (Figures 3E and 3F). In addition, a time course experiment of HSV-1 infection in HeLa cells showed very similar changes in size and number of P-bodies (Figures S3A and S3B). Interestingly, when we analyzed gene expression data from an HSV-1 infection time course, we found that the m6A-dependent depletion of host mRNAs occurred at a time point shortly after the onset of P-body reorganization (Figures S3A–S3C).

Taken together, these data show that alphaherpesvirus infection-induced selective depletion of m6A-containing transcripts correlates with YTHDF protein localization into fewer but larger P-bodies.

Preferential degradation of m6A-methylated transcripts does not depend on the UL41/vhs viral RNAse

Next, we wanted to identify the stage of viral infection that is associated with P-body reorganization and increased destabilization of m6A-containing transcripts during PRV infection. Herpesvirus infection consists of viral entry in the host cell, viral genome delivery and replication in the nucleus and viral gene expression

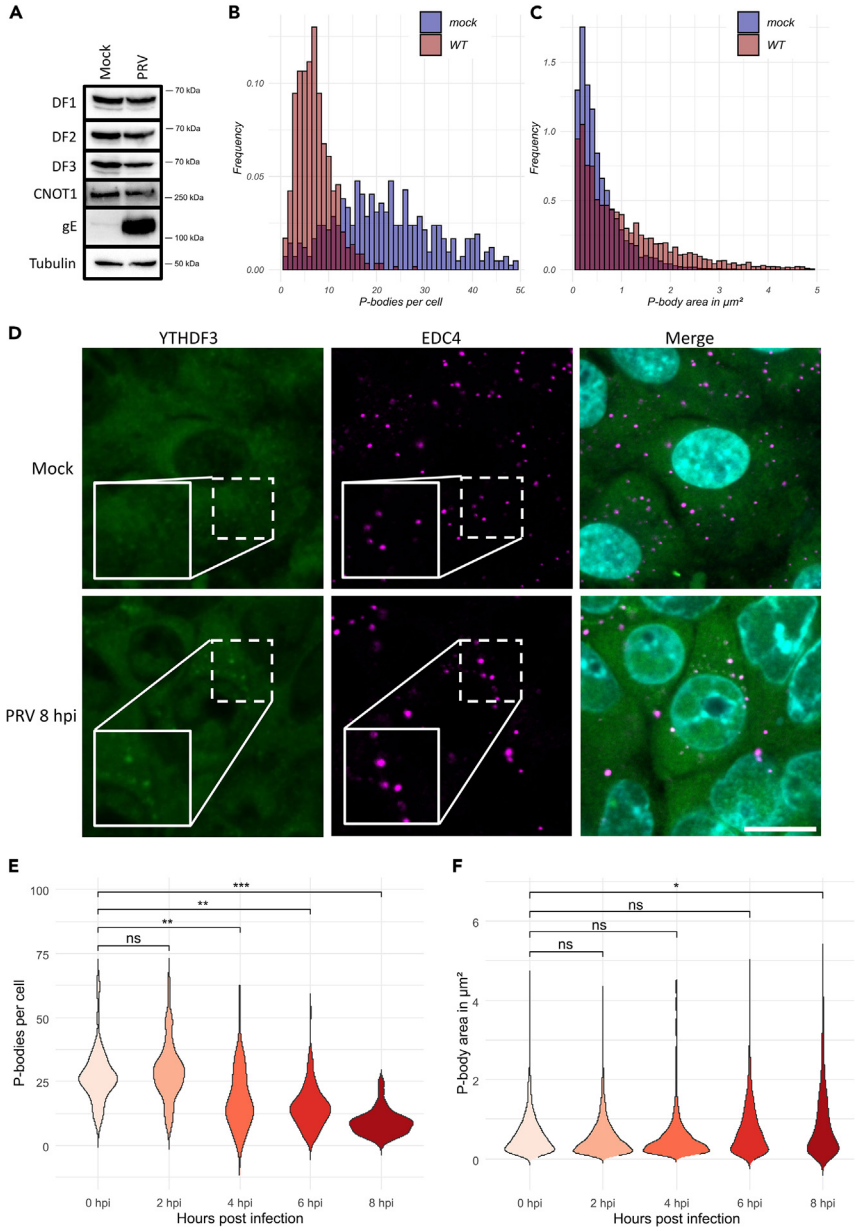

Figure 3. Subcellular localization of YTHDF proteins and P-body reorganization in PRV-infected cells

(A) Western blot analysis of the YTHDF (DF) proteins and CNOT1 in mock- or PRV-infected ST cells (MOI of 10, 16 hpi).

(B and C) Distribution of the number (B) and size (C) of P-bodies in mock- or PRV-infected cells (MOI of 10, 8 hpi).

(D) Immunofluorescence staining of YTHDF3 and the P-body marker EDC4 in mock- or PRV-infected ST cells (MOI of 10, 8 hpi). Scale bar, 15 µm.

(E and F) Distribution of the number (n = 450) (E) and size (n = 7748) (F) of P-bodies over time in PRV-infected ST cells (MOI of 10). *p < 0.05, **p < 0.01, ***p < 0.001, ****p < 0.0001.

which is organized in a transcriptional cascade starting with immediate-early genes, including genes encoding transcription factors that activate the transcription of early genes.[48,49] These early genes then encode proteins required, among others, for replication of the viral genome. The production of viral genomes is the trigger for the expression of late genes that mostly encode structural components of the virion.[48,49]

In order to narrow down the infection stage responsible for the observed effects, we asked if the effect of PRV and HSV-1 infection on P-bodies occurs during virus entry in the host cell. To test this, we quantified

P-body size and number in cells infected with UV-inactivated PRV or HSV-1. UV-inactivated virus is able to enter host cells but is unable to initiate viral gene expression. P-bodies in cells infected with UV-inactivated virus were similar to those in mock-infected cells, indicating that proteins associated with the incoming virus are not sufficient to alter P-bodies, and that viral gene expression is required for this process (Figures 4A, 4B, S3D, and S3E).

We next examined whether P-body changes occur prior to the viral genome replication step. To test this, we monitored P-bodies in PRV- or HSV-1-infected cells treated with phosphono-acetic acid (PAA). PAA selectively blocks viral genome replication, thus preventing the expression of late viral genes. Whereas PAA treatment partially blocked PRV-induced P-body remodeling (Figures 4A and 4B), it did not significantly affect HSV-1-induced P-body remodeling (Figures S3D and S3E). However, analysis of a publicly available RNA-seq dataset of HSV-1-infected fibroblasts that were either or not treated with PAA showed that PAA treatment largely inhibited the selective depletion of m6A-containing transcripts (Figure S3F). These data indicate that, whereas HSV-1-induced P-body changes depend mostly on expression of early viral factors, depletion of m6A-containing transcripts depends largely on viral genome replication and/or late viral protein expression.

When considering potential viral factors that may be involved in virus-induced depletion of m6A-methylated transcripts, a particularly notable protein is UL41, a viral protein that contains RNase activity and is encoded by all alphaherpesviruses.[50–53] UL41 is also called the virion host shutoff protein (vhs) and plays an important role in virus-induced host shutdown. UL41/vhs is a structural component that may function during virus entry of the host cell and/or late in infection of the host cell, as UL41/vhs is expressed as a late gene in infected cells.[50–53] The RNase activity of UL41/vhs has been described as relatively nonspecific and corresponds to that of RNase A.[54] Nevertheless, to confirm whether or not UL41/vhs is involved in P-body rearrangements and/or depletion of m6A-methylated transcripts, we first analyzed a GEO dataset containing RNA-seq data from HepG2 cells infected with isogenic wild-type HSV-1 or HSV-1 lacking the UL41/vhs protein. UL41null HSV-1 infection induced a preferential degradation of m6A containing transcripts that was largely similar to that observed in wild-type HSV-1 infected cells (Figures 4C and 4D), indicating that UL41/vhs is not essential for the preferential destabilization of m6A-containing transcripts. In line with this, we found that P-body reorganization was similar in cells infected with UL41null PRV or UL41-null HSV-1 compared to cells infected with the corresponding wild-type virus (Figure S4).

In conclusion, PRV- and HSV-1-induced changes in P-bodies require *de novo* viral gene expression, and P-body reorganization and preferential depletion of m6A-containing transcripts are independent of the viral RNAse UL41/vhs.

YTHDF knockdown does not abrogate viral replication in cell culture, but suppresses PRV protein production and triggers increased expression of ISGs in primary porcine epithelial cells

We next wanted to investigate the potential contribution of preferential destabilization of m6A-methylated transcripts in the context of viral infection. We therefore prevented selective degradation of m6A-containing transcripts by knocking down the YTHDF proteins in ST cells, and subsequently infected the cells with PRV and analyzed production of viral proteins and viral titers. Knockdown of the YTHDF proteins did not affect expression of the early viral protein US3 and only slightly reduced expression of the late viral protein gE in ST cells (Figure 5A). In line with this, YTHDF protein depletion did not significantly affect production of infectious virus in PRV-infected ST cells (Figure 5B).

m6A is enriched in transcripts that regulate the type I interferon response, including STAT1, IRF1, IFNB,[9,10,12] and numerous ISGs, including IFITM1 and MX1 [11]. Thus, m6A methylation has been shown to be a crucial regulator of the antiviral type I IFN response.[9,10] Examination of RNA-seq data and RT-qPCR showed that ST cells, like many immortalized cell lines,[55] are defective in type I IFN production. In line with this, siRNA-mediated knock down of the YTHDF proteins in ST cells did not result in detectable IFN/ISG expression (data not shown). Hence, any effects of YTHDF-mediated selective degradation of m6A-containing transcripts on the production of type I IFN and interferon-stimulated genes (ISGs) cannot be readily assessed in this cell type.

Therefore, we examined ISG expression after PRV infection in isolated primary porcine kidney (PPK) cells. We examined the expression of *ISG15*, *ISG54*, and *2′5′OAS* using RT-qPCR. After PRV infection of PPK cells, we observed reduced expression of these transcripts, compared to their expression in mock-infected cells,

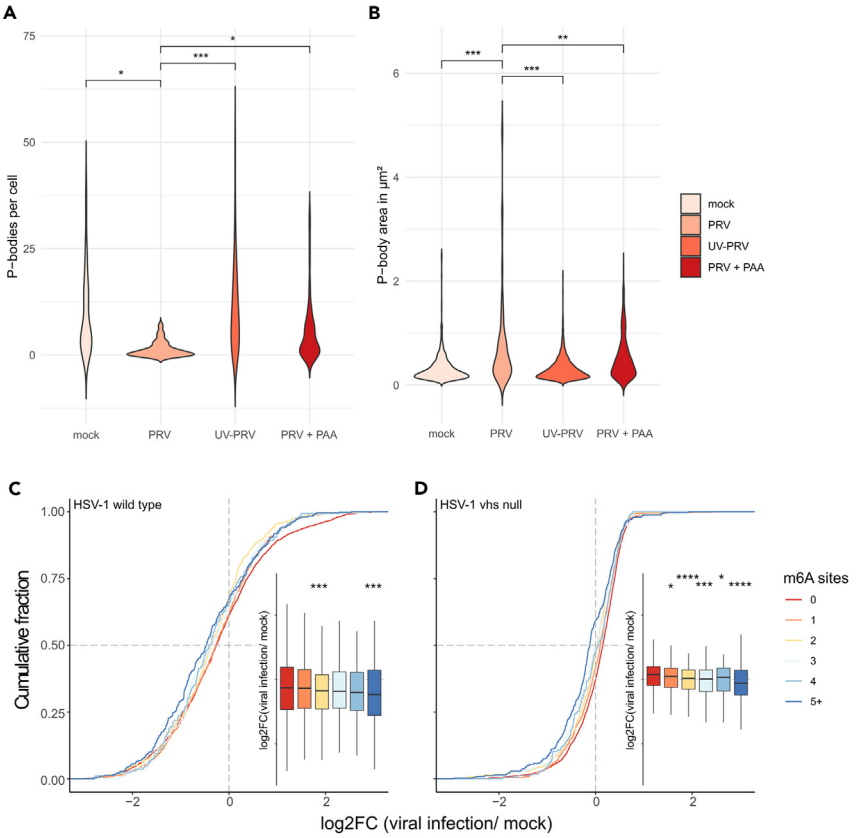

Figure 4. Changes in P-bodies during PRV or HSV-1 infection are triggered post virus entry and do not depend on UL41/vhs

(A and B) Distribution of the number (n = 260) (A) and size (n = 1883) (B) of P-bodies in ST cells infected with wild type PRV, UV-inactivated PRV or infected with PRV at an MOI of 10 in the presence of phosphonoacetic acid (PAA) at 8 hpi.

(C and D) Cumulative fold change of transcripts as measured by RNA-seq between mock and HSV-1-infected HFF cells at an MOI of 10 at 8 hpi for wild type (C) or vhsnull (D) HSV-1. The transcripts expressed in each cell line were binned based on the expected number of m6A sites per transcript based on previous m6A maps. *p < 0.05, **p < 0.01, ***p < 0.001, ****p < 0.0001.

consistent with degradation of these transcripts induced by PRV infection (Figure 5C). We next performed YTHDF depletion by knockdown of YTHDF1, 2, and 3 in PPK cells (Figures 5C and 5D). RT-qPCR showed that depletion of YTHDF proteins in PKK cells induced a marked increase in the expression of ISGs in both mock- and PRV-infected cells (Figure 5C). In addition, whereas in PPK cells treated with scrambled siRNA, the mRNA expression levels of ISG54 were significantly reduced in PRV-infected cells compared to mock-infected cells, this was not the case in PRV-infected cells lacking YTHDF proteins (Figure 5C). Overall, these results are consistent with a role of YTHDF proteins in mediating suppression of ISG transcripts upon PRV infection.

We next asked if the increase in ISG expression observed in YTHDF siRNA-treated PPK cells correlates with suppressed PRV viral protein production. Indeed, unlike in IFN-deficient ST cells (see Figure 5A), depletion of YTHDF proteins in PPK cells resulted in a substantial reduction of PRV protein production (Figure 5D). Thus, YTHDF function is needed for efficient PRV viral protein production in interferon-expressing primary cells. Overall, these findings are consistent with our observations that during PRV infection, YTHDF proteins drive degradation of m6A-containing transcripts, which include transcripts encoding regulators of the type I interferon response, thus enabling efficient viral replication.

DISCUSSION

Despite the increasing body of recent research regarding the presence and function of m6A methylation in viral transcripts,[15–18,56–62] less attention has gone to the impact of virus infection on the global fate of cellular

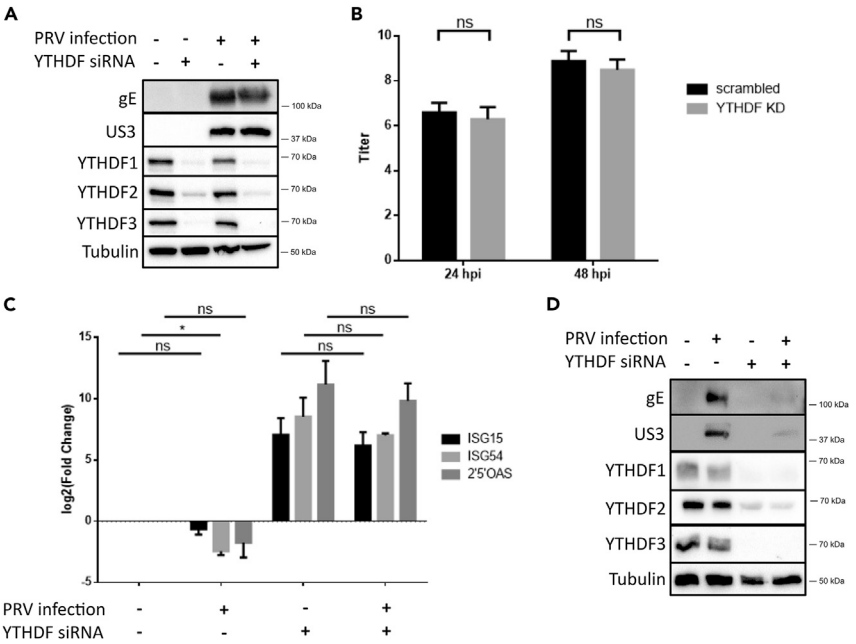

Figure 5. Influence of YTHDF knockdown on PRV replication and the antiviral type I IFN response

(A) Western blot analysis of viral proteins gE and US3 in ST cells that were mock-infected or infected with PRV for 16 h upon 48 h of siRNA-mediated knockdown of the three YTHDF proteins or transfection with a scrambled siRNA (n = 3). Quantification of western blots indicated that, upon normalization to the tubulin protein control, all YTHDF-targeted siRNA treatments in ST cells reached an efficiency of ≥ 73% target protein reduction.

(B) Viral titers at 24 and 48 hpi in PRV-infected ST cells, inoculated (MOI of 10) upon 48 h of siRNA-mediated knockdown of the three YTHDF proteins or treatment with scrambled siRNA (n = 3).

(C) RT-qPCR of different ISGs in mock- or PRV-infected PPK cells, inoculated (MOI of 10) upon 48 h of siRNA-mediated knockdown of the three YTHDF proteins or treatment with scrambled siRNA (n = 4). *$p < 0.05$.

(D) Western blot analysis of viral proteins gE and US3 in PPK cells that were mock-infected or infected with PRV (MOI of 10) for 16 h upon 48 h of siRNA-mediated knockdown of the three YTHDF proteins or treatment with scrambled siRNA (n = 3). Quantification of western blots indicated that, upon normalization to the tubulin protein control, all YTHDF-targeted siRNA treatments in PPK cells reached an efficiency of ≥ 81% target protein reduction.

m6A-methylated transcripts. Here, we systematically screened existing RNA-seq datasets of cells infected with viruses from different virus families to determine the effect of viral infection on m6A-methylated transcripts. We took advantage of the high conservation of m6A sites between different cell types to use existing m6A maps to infer the methylation level of transcripts. Although infection with most viruses that were analyzed does not specifically affect m6A-methylated transcripts, several viruses triggered a specific up- or downregulation of m6A-containing transcripts. Specific alphaherpesviruses (but not beta- or gammaherpesviruses), Sendai virus and African swine fever virus trigger a selective downregulation of m6A-methylated transcripts. Using the porcine alphaherpesvirus PRV, we show that this process is mediated by YTHDF proteins and that knockdown of YTHDF proteins results in increased expression of interferon-stimulated genes (ISGs) and reduced viral protein production in interferon-competent primary porcine epithelial cells.

For PRV, we found that the selective destabilization of m6A-containing transcripts depends on the cellular YTHDF m6A reader proteins and correlates with a localization of the YTHDF proteins to reorganized P-bodies. Although our results are in line with the general notion that degradation of m6A-methylated transcripts is a major, if not the key, function of YTHDF proteins, the EISA data (Figure S1) should be interpreted with caution, as any type of treatment may affect proteins involved in global regulation of the mRNA life cycle.[46] This is likely the case for virus infection and could therefore be considered as a potential limitation of this part of the study. Hence, future assays using alternative approaches and methods may further substantiate the indications provided by the EISA data. Regardless, we observed that during PRV infection, P-bodies are fewer in number but larger in size, possibly increasing the efficiency of mRNA degradation. The induction of larger P-bodies was previously described in HSV-1-infected HeLa cells, but its function remained unclear.[52] Infection with UV-inactivated virus and infection in the presence of PAA showed that the

changes in P-bodies do not occur during virus entry and do not (for HSV-1) or do at least partly (for PRV) depend on viral genome replication. Further, at least in HSV-1, virus-induced depletion of m6A-containing transcripts largely depends on viral genome replication/viral late gene expression. Hence, whereas, in the case of HSV-1, virus-induced P-body rearrangements are triggered predominantly by early viral factors, depletion of m6A-containing transcripts requires contribution of additional, late viral factors and the host YTHDF proteins, which show increased co-localization with P-bodies. Future research will need to resolve the molecular mechanisms used by alphaherpesviruses to trigger reorganization of P-bodies and if and how this affects P-body and YTHDF functionality. Since m6A enhances the phase separation potential of transcripts through YTHDF proteins,[47] one potential hypothesis could be that phase separation may be involved in a virus-mediated fusion process of P-bodies, which will be addressed in follow-up studies. In this context, it may be of interest that some HSV-1 proteins have been reported to drive or undergo liquid-liquid phase separation, including the immediate-early protein ICP4 and the late protein UL11.[63,64] It will be interesting to investigate if these, or other, intrinsically disordered viral proteins contribute to the virus-induced P-body rearrangement and/or depletion of m6A-containing transcripts that we describe here.

Knockdown of the YTHDF readers blocked PRV infection-induced degradation of m6A-containing transcripts, but did not substantially inhibit viral replication in the (interferon deficient) ST cell line. This suggests that alphaherpesvirus-induced preferential degradation of m6A-containing transcripts is not directly involved in the virus replication cycle. However, knockdown of the YTHDF proteins resulted in increased type I ISG expression levels in interferon expressing primary cells, pointing toward degradation of m6A-containing transcripts as a viral IFN evasion mechanism. These findings are in line with accumulating evidence that m6A modification of RNA is crucial in the regulation of the immune system, and particularly that type I IFN and ISG transcripts are m6A-methylated.[9–11,65] Our data also provide additional convincing evidence that YTHDF m6A readers are important regulators of the magnitude of the type I IFN response, in line with recent data.[9,66] Hence, it may be interesting to investigate whether altered YTHDF activity may contribute to certain pathologies, including type I IFN autoimmune diseases.[67] In addition, many other immune response-related cytokine- and cytokine-receptor-encoding transcripts are also m6A-modified, suggesting that the implications of virus-mediated degradation of m6A-containing transcripts may stretch beyond the type I IFN response.[7,8,36,65]

Notably, PRV and HSV-1 infection affects the m6A pathway in different ways. As shown here, infection with these viruses is associated with degradation of m6A-methylated host mRNAs via YTHDF proteins. On the other hand, we and others have shown that PRV and HSV-1 inactivate the m6A writer complex.[68–72] Our current hypothesis is that both mechanisms complement each other to allow optimized viral gene expression while suppressing the antiviral host cell response. Indeed, viral inhibition of the m6A writer complex occurs at a relatively late stage in host cell infection,[69,71] when newly transcribed mRNAs are virtually exclusively viral mRNAs.[73,74] Hence, viral inhibition of the m6A writer complex at a time point when transcription is focused on viral gene expression will protect these viral transcripts from the YTHDF-mediated degradation that we describe here, while the preferential degradation of m6A-methylated host transcripts does affect transcripts that are involved in the rapid antiviral type I interferon response by the host cell. In addition, we reported earlier that the DRACH m6A methylation sequence is significantly under-represented in the viral genome of alphaherpesviruses, but not in that of beta- or gammaherpesviruses,[71] which we interpret as an additional safeguard system by these viruses to avoid YTHDF-mediated degradation of their own viral transcripts. Such an elegant, coordinated response would allow these alphaherpesviruses to maximally utilize the m6A pathway for their own benefit. Additional studies will be targeted at further addressing this hypothesis.

In conclusion, our data describe a previously uncharacterized impact of specific alphaherpesviruses on the host epitranscriptome, consisting of the degradation of m6A-containing transcripts via the YTHDF m6A reader proteins. YTHDF-mediated degradation of m6A-containing transcripts suppresses expression of ISGs, indicating that alphaherpesvirus-mediated degradation of m6A-containing transcripts represents a viral IFN evasion strategy.

Limitations of the study

As indicated in the discussion, although our results are in line with the general notion that YTHDF proteins drive degradation of m6A-methylated transcripts, the EISA data should be interpreted with caution, as any type of treatment (including virus infection) may affect proteins involved in global regulation of the mRNA life cycle.[46] Future assays that make use of alternative methodology may further substantiate the EISA-based indications provided in the current study. Further, although we observed a correlation between

YTHDF-mediated depletion of m6A-containing host transcripts and increased localization of YTHDF proteins to enlarged P-bodies in virus-infected cells, this does not necessarily reflect a causal relationship between both sets of observations. Future assays directed at identifying the viral factors that drive both phenotypes will allow to further assess a potential causal relationship. Also, some of our findings are in line with and thereby further confirm earlier studies, in particular the contribution of YTHDF proteins to degradation of m6A-containing transcripts, the role of YTHDF proteins in regulating type I interferon responses and ISG expression and the location of YTHDF proteins to P-bodies.[9,40,41,47,66]

STAR★METHODS

Detailed methods are provided in the online version of this paper and include the following:

- KEY RESOURCES TABLE
- RESOURCE AVAILABILITY
  - Lead contact
  - Materials availability
  - Data and code availability
- EXPERIMENTAL MODEL AND STUDY PARTICIPANT DETAILS
  - Cells and viruses
- METHOD DETAILS
  - Sequencing and analysis
  - M6A reader knockdown
  - Cell treatments
  - Immunofluorescence
  - Western blotting
  - Virus titrations
  - RNA isolation and real time quantitative PCR (RT-qPCR)
  - Graphic illustrations
- QUANTIFICATION AND STATISTICAL ANALYSIS

SUPPLEMENTAL INFORMATION

Supplemental information can be found online at https://doi.org/10.1016/j.isci.2023.107310.

ACKNOWLEDGMENTS

We would like to thank Cliff Van Waesberghe for excellent technical assistance, the NXTGNT genome analysis service facility for generating the sequencing data, Leigh Anne Olsen and Lynn Enquist (Princeton University, Princeton, USA) for their kind gift of anti-PRV US3 monoclonal antibodies and the ID-DLO (The Netherlands) for the NIA3 PRV strain. This project was supported by grants from F.W.O.-Vlaanderen (G060119N), the Special Research Fund of Ghent University (Concerted research grants GOA013-17 and GOA015-23) (H.W.F.), a grant from the Belgian American Education Foundation (BAEF) (R.J.J.J.), and NIH grants R35 NS111631 (S.R.J.) and T32 CA062948 (A.O.-G).

AUTHOR CONTRIBUTIONS

Conceptualization, R.J.J.J., A.O.G., S.J., and H.W.F.; Formal Analysis, R.J.J.J., A.O.G., and R.V.; Investigation, R.J.J.J., R.V., and A.M.; Resources, S.J. and H.W.F.; Writing – Original draft, R.J.J.J. and H.W.F., Writing – Review and Editing, R.J.J.J., A.O.G., R.V., A.M., S.J., and H.W.F.; Visualization, R.J.J.J. and A.O.G., Supervision, A.O.G., S.J., and H.W.F.; Project administration, H.W.F.; Funding acquisition, A.O.G., S.J., and H.W.F.

DECLARATION OF INTERESTS

S.J. is an advisor to, and owns equity in 858 Therapeutics and Lucerna Technologies.

Received: January 25, 2023
Revised: June 4, 2023
Accepted: July 4, 2023
Published: July 10, 2023

REFERENCES

1. Rivas, H.G., Schmaling, S.K., and Gaglia, M.M. (2016). Shutoff of host gene expression in influenza A virus and herpesviruses: Similar mechanisms and common themes. Viruses *8*, 102–126. https://doi.org/10.3390/v8040102.

2. Esclatine, A., Taddeo, B., and Roizman, B. (2004). The UL41 protein of herpes simplex virus mediates selective stabilization or degradation of cellular mRNAs. Proc. Natl. Acad. Sci. USA *101*, 18165–18170. https://doi.org/10.1073/pnas.0408272102.

3. Taddeo, B., Esclatine, A., Zhang, W., and Roizman, B. (2003). The Stress-Inducible Immediate-Early Responsive Gene IEX-1 Is Activated in Cells Infected with Herpes Simplex Virus 1, but Several Viral Mechanisms, Including 3′ Degradation of Its RNA, Preclude Expression of the Gene. J. Virol. *77*, 6178–6187. https://doi.org/10.1128/jvi.77.11.6178-6187.2003.

4. Gaglia, M.M., Rycroft, C.H., and Glaunsinger, B.A. (2015). Transcriptome-Wide Cleavage Site Mapping on Cellular mRNAs Reveals Features Underlying Sequence-Specific Cleavage by the Viral Ribonuclease SOX. PLoS Pathog. *11*, e1005305–e1005325. https://doi.org/10.1371/journal.ppat.1005305.

5. Rodriguez, A., Pérez-González, A., and Nieto, A. (2007). Influenza Virus Infection Causes Specific Degradation of the Largest Subunit of Cellular RNA Polymerase II. J. Virol. *81*, 5315–5324. https://doi.org/10.1128/jvi.02129-06.

6. Murakami, S., and Jaffrey, S.R. (2022). Hidden codes in mRNA: Control of gene expression by m6A. Mol. Cell *82*, 2236–2251. https://doi.org/10.1016/j.molcel.2022.05.029.

7. Meyer, K.D., Saletore, Y., Zumbo, P., Elemento, O., Mason, C.E., and Jaffrey, S.R. (2012). Comprehensive Analysis of mRNA Methylation Reveals Enrichment in 3′ UTRs and near Stop Codons. Cell *149*, 1635–1646. https://doi.org/10.1016/j.cell.2012.05.003.

8. Dominissini, D., Moshitch-Moshkovitz, S., Schwartz, S., Salmon-Divon, M., Ungar, L., Osenberg, S., Cesarkas, K., Jacob-Hirsch, J., Amariglio, N., Kupiec, M., et al. (2012). Topology of the human and mouse m6A RNA methylomes revealed by m6A-seq. Nature *485*, 201–206. https://doi.org/10.1038/nature11112.

9. Winkler, R., Gillis, E., Lasman, L., Safra, M., Geula, S., Soyris, C., Nachshon, A., Tai-Schmiedel, J., Friedman, N., Le-Trilling, V.T.K., et al. (2019). m6A modification controls the innate immune response to infection by targeting type I interferons. Nat. Immunol. *20*, 173–182. https://doi.org/10.1038/s41590-018-0275-z.

10. Rubio, R.M., Depledge, D.P., Bianco, C., Thompson, L., and Mohr, I. (2018). RNA m 6 A modification enzymes shape innate responses to DNA by regulating interferon β. Genes Dev. *32*, 1472–1484. https://doi.org/10.1101/gad.319475.118.

11. McFadden, M.J., McIntyre, A.B.R., Mourelatos, H., Abell, N.S., Gokhale, N.S., Ipas, H., Xhemalçe, B., Mason, C.E., and Horner, S.M. (2021). Post-transcriptional regulation of antiviral gene expression by N6-methyladenosine. Cell Rep. *34*, 108798. https://doi.org/10.1016/j.celrep.2021.108798.

12. Wang, L., Hui, H., Agrawal, K., Kang, Y., Li, N., Tang, R., Yuan, J., and Rana, T.M. (2020). m 6 A RNA methyltransferases METTL3/14 regulate immune responses to anti-PD-1 therapy. EMBO J. *39*, e104514–e104515. https://doi.org/10.15252/embj.2020104514.

13. Zaccara, S., Ries, R.J., and Jaffrey, S.R. (2019). Reading, writing and erasing mRNA methylation. Nat. Rev. Mol. Cell Biol. *20*, 608–624. https://doi.org/10.1038/s41580-019-0168-5.

14. Kim, G.-W., Imam, H., Khan, M., and Siddiqui, A. (2020). N 6 -Methyladenosine modification of hepatitis B and C viral RNAs attenuates host innate immunity via RIG-I signaling. J. Biol. Chem. *295*, 13123–13133. https://doi.org/10.1074/jbc.ra120.014260.

15. Lu, M., Zhang, Z., Xue, M., Zhao, B.S., Harder, O., Li, A., Liang, X., Gao, T.Z., Xu, Y., Zhou, J., et al. (2020). N 6-methyladenosine modification enables viral RNA to escape recognition by RNA sensor RIG-I. Nat. Microbiol. *5*, 584–598. https://doi.org/10.1038/s41564-019-0653-9.

16. Tsai, K., Courtney, D.G., and Cullen, B.R. (2018). Addition of m6A to SV40 late mRNAs enhances viral structural gene expression and replication. PLoS Pathog. *14*, e1006919–e1006923. https://doi.org/10.1371/journal.ppat.1006919.

17. Courtney, D.G., Kennedy, E.M., Dumm, R.E., Bogerd, H.P., Tsai, K., Heaton, N.S., and Cullen, B.R. (2017). Epitranscriptomic Enhancement of Influenza A Virus Gene Expression and Replication. Cell Host Microbe *22*, 377–386.e5. https://doi.org/10.1016/j.chom.2017.08.004.

18. Kennedy, E.M., Bogerd, H.P., Kornepati, A.V.R., Kang, D., Ghoshal, D., Marshall, J.B., Poling, B.C., Tsai, K., Gokhale, N.S., Horner, S.M., and Cullen, B.R. (2016). Posttranscriptional m6A Editing of HIV-1 mRNAs Enhances Viral Gene Expression. Cell Host Microbe *19*, 675–685. https://doi.org/10.1016/j.chom.2016.04.002.

19. De Maio, F.A., Risso, G., Iglesias, N.G., Shah, P., Pozzi, B., Gebhard, L.G., Mammi, P., Mancini, E., Yanovsky, M.J., Andino, R., et al. (2016). The Dengue Virus NS5 Protein Intrudes in the Cellular Spliceosome and Modulates Splicing. PLoS Pathog. *12*, e10058411. https://doi.org/10.1371/journal.ppat.1005841.

20. Lee, E.Y., Lee, H.C., Kim, H.K., Jang, S.Y., Park, S.J., Kim, Y.H., Kim, J.H., Hwang, J., Kim, J.H., Kim, T.H., et al. (2016). Infection-specific phosphorylation of glutamyl-prolyl tRNA synthetase induces antiviral immunity. Nat. Immunol. *17*, 1252–1262. https://doi.org/10.1038/ni.3542.

21. Gamage, A.M., Tan, K.S., Chan, W.O.Y., Liu, J., Tan, C.W., Ong, Y.K., Thong, M., Andiappan, A.K., Anderson, D.E., Wang, D.Y., and Wang, L.F. (2020). Infection of human Nasal Epithelial Cells with SARS-CoV-2 and a 382-nt deletion isolate lacking ORF8 reveals similar viral kinetics and host transcriptional profiles. PLoS Pathog. *16*, e10091300. https://doi.org/10.1371/journal.ppat.1009130.

22. Li, Y., Zhong, C., Liu, D., Yu, W., Chen, W., Wang, Y., Shi, S., and Yuan, Y. (2018). Evidence for Kaposi sarcoma originating from mesenchymal stem cell through KSHV-induced mesenchymal-to-endothelial transition. Cancer Res. *78*, 230–245. https://doi.org/10.1158/0008-5472.CAN-17-1961.

23. Batra, R., Stark, T.J., Clark, A.E., Belzile, J.P., Wheeler, E.C., Yee, B.A., Huang, H., Gelboin-Burkhart, C., Huelga, S.C., Aigner, S., et al. (2016). RNA-binding protein CPEB1 remodels host and viral RNA landscapes. Nat. Struct. Mol. Biol. *23*, 1101–1110. https://doi.org/10.1038/nsmb.3310.

24. Pheasant, K., Möller-Levet, C.S., Jones, J., Depledge, D., Breuer, J., and Elliott, G. (2018). Nuclear-cytoplasmic compartmentalization of the herpes simplex virus 1 infected cell transcriptome is co-ordinated by the viral endoribonuclease vhs and cofactors to facilitate the translation of late proteins. PLoS Pathog. *14*, e1007331. https://doi.org/10.1371/journal.ppat.1007331.

25. Long, X., Yang, J., Zhang, X., Yang, Z., Li, Y., Wang, F., Li, X., and Kuang, E. (2021). BRLF1 suppresses RNA Pol III-mediated RIG-I inflammasome activation in the early EBV lytic lifecycle. EMBO Rep. *22*, e50714–e50718. https://doi.org/10.15252/embr.202050714.

26. Wyler, E., Menegatti, J., Franke, V., Kocks, C., Boltengagen, A., Hennig, T., Theil, K., Rutkowski, A., Ferrai, C., Baer, L., et al. (2017). Widespread activation of antisense transcription of the host genome during herpes simplex virus 1 infection. Genome Biol. *18*, 209–219. https://doi.org/10.1186/s13059-017-1329-5.

27. Yuan, S., Liao, G., Zhang, M., Zhu, Y., Xiao, W., Wang, K., Li, C., Jia, C., Sun, N., Walch, A., et al. (2021). Multiomics interrogation into HBV (Hepatitis B virus)-host interaction reveals novel coding potential in human genome, and identifies canonical and non-canonical proteins as host restriction factors against HBV. Cell Discov. *7*, 105. https://doi.org/10.1038/s41421-021-00337-3.

28. Full, F., van Gent, M., Sparrer, K.M.J., Chiang, C., Zurenski, M.A., Scherer, M., Brockmeyer, N.H., Heinzerling, L., Stürzl, M., Korn, K., et al. (2019). Centrosomal protein TRIM43 restricts herpesvirus infection by regulating nuclear lamina integrity. Nat. Microbiol. *4*, 164–176. https://doi.org/10.1038/s41564-018-0285-5.

29. Hennig, T., Michalski, M., Rutkowski, A.J., Djakovic, L., Whisnant, A.W., Friedl, M.S., Jha, B.A., Baptista, M.A.P., L'Hernault, A., Erhard, F., et al. (2018). HSV-1-induced disruption of transcription termination resembles a cellular

stress response but selectively increases chromatin accessibility downstream of genes. PLoS Pathog. *14*, e10069544. https://doi.org/10.1371/journal.ppat.1006954.

30. Rutkowski, A.J., Erhard, F., L'Hernault, A., Bonfert, T., Schilhabel, M., Crump, C., Rosenstiel, P., Efstathiou, S., Zimmer, R., Friedel, C.C., and Dölken, L. (2015). Widespread disruption of host transcription termination in HSV-1 infection. Nat. Commun. *6*, 7126. https://doi.org/10.1038/ncomms8126.

31. Friedel, C.C., Whisnant, A.W., Djakovic, L., Rutkowski, A.J., Friedl, M.-S., Kluge, M., Williamson, J.C., Sai, S., Vidal, R.O., Sauer, S., et al. (2021). Dissecting Herpes Simplex Virus 1-Induced Host Shutoff at the RNA Level. J. Virol. *95*, e01399-20. https://doi.org/10.1128/jvi.01399-20.

32. Sundaramoorthy, E., Ryan, A.P., Fulzele, A., Leonard, M., Daugherty, M.D., and Bennett, E.J. (2021). Ribosome quality control activity potentiates vaccinia virus protein synthesis during infection. J. Cell Sci. *134*, jcs257188. https://doi.org/10.1242/jcs.257188.

33. Nogalski, M.T., Solovyov, A., Kulkarni, A.S., Desai, N., Oberstein, A., Levine, A.J., Ting, D.T., Shenk, T., and Greenbaum, B.D. (2019). A tumor-specific endogenous repetitive element is induced by herpesviruses. Nat. Commun. *10*, 90. https://doi.org/10.1038/s41467-018-07944-x.

34. Dierks, D., Garcia-Campos, M.A., Uzonyi, A., Safra, M., Edelheit, S., Rossi, A., Sideri, T., Varier, R.A., Brandis, A., Stelzer, Y., et al. (2021). Multiplexed profiling facilitates robust m6A quantification at site, gene and sample resolution. Nat. Methods *18*, 1060–1067. https://doi.org/10.1038/s41592-021-01242-z.

35. Ke, S., Pandya-Jones, A., Saito, Y., Fak, J.J., Vågbø, C.B., Geula, S., Hanna, J.H., Black, D.L., Darnell, J.E., and Darnell, R.B. (2017). m 6 A mRNA modifications are deposited in nascent pre-mRNA and are not required for splicing but do specify cytoplasmic turnover. Genes Dev. *31*, 990–1006. https://doi.org/10.1101/gad.301036.117.

36. Linder, B., Grozhik, A.V., Olarerin-George, A.O., Meydan, C., Mason, C.E., and Jaffrey, S.R. (2015). Single-nucleotide-resolution mapping of m6A and m6Am throughout the transcriptome. Nat. Methods *12*, 767–772. https://doi.org/10.1038/nmeth.3453.

37. Wu, S., Yang, S., Ou, M., Chen, J., Huang, J., Xiong, D., Sun, W., and Xiao, L. (2021). Transcriptome Analysis Reveals the Role of Cellular Calcium Disorder in Varicella Zoster Virus-Induced Post-Herpetic Neuralgia. Front. Mol. Neurosci. *14*, 665931. https://doi.org/10.3389/fnmol.2021.665931.

38. Gomi, Y., Sunamachi, H., Mori, Y., Nagaike, K., Takahashi, M., and Yamanishi, K. (2002). Comparison of the complete DNA sequences of the Oka varicella vaccine and its parental virus. J. Virol. *76*, 11447–11459. https://doi.org/10.1128/jvi.76.22.11447-11459.2002.

39. Pomeranz, L.E., Reynolds, A.E., and Hengartner, C.J. (2005). Molecular Biology of Pseudorabies Virus: Impact on Neurovirology and Veterinary Medicine. Microbiol. Mol. Biol. Rev. *69*, 462–500. https://doi.org/10.1128/mmbr.69.3.462-500.2005.

40. Wang, X., Lu, Z., Gomez, A., Hon, G.C., Yue, Y., Han, D., Fu, Y., Parisien, M., Dai, Q., Jia, G., et al. (2014). N6-methyladenosine-dependent regulation of messenger RNA stability. Nature *505*, 117–120. https://doi.org/10.1038/nature12730.

41. Zaccara, S., and Jaffrey, S.R. (2020). A Unified Model for the Function of YTHDF Proteins in Regulating m6A-Modified mRNA. Cell *181*, 1582–1595.e18. https://doi.org/10.1016/j.cell.2020.05.012.

42. Patil, D.P., Pickering, B.F., and Jaffrey, S.R. (2018). Reading m6A in the Transcriptome: m6A-Binding Proteins. Trends Cell Biol. *28*, 113–127. https://doi.org/10.1016/j.tcb.2017.10.001.

43. Shi, H., Wang, X., Lu, Z., Zhao, B.S., Ma, H., Hsu, P.J., Liu, C., and He, C. (2017). YTHDF3 facilitates translation and decay of N6-methyladenosine-modified RNA. Cell Res. *27*, 315–328. https://doi.org/10.1038/cr.2017.15.

44. Wang, X., Zhao, B.S., Roundtree, I.A., Lu, Z., Han, D., Ma, H., Weng, X., Chen, K., Shi, H., and He, C. (2015). N6-methyladenosine modulates messenger RNA translation efficiency. Cell *161*, 1388–1399. https://doi.org/10.1016/j.cell.2015.05.014.

45. Lasman, L., Krupalnik, V., Viukov, S., Mor, N., Aguilera-Castrejon, A., Schneir, D., Bayerl, J., Mizrahi, O., Peles, S., Tawil, S., et al. (2020). Context-dependent functional compensation between Ythdf m6A reader proteins. Genes Dev. *34*, 1373–1391. https://doi.org/10.1101/gad.340695.120.

46. Gaidatzis, D., Burger, L., Florescu, M., and Stadler, M.B. (2015). Analysis of intronic and exonic reads in RNA-seq data characterizes transcriptional and post-transcriptional regulation. Nat. Biotechnol. *33*, 722–729. https://doi.org/10.1038/nbt.3269.

47. Ries, R.J., Zaccara, S., Klein, P., Olarerin-George, A., Namkoong, S., Pickering, B.F., Patil, D.P., Kwak, H., Lee, J.H., and Jaffrey, S.R. (2019). m6A enhances the phase separation potential of mRNA. Nature *571*, 424–428. https://doi.org/10.1038/s41586-019-1374-1.

48. Honess, R.W., and Roizman, B. (1974). Regulation of Herpesvirus Macromolecular Synthesis I. Cascade Regulation of the Synthesis of Three Groups of Viral Proteins 1. J. Virol. *14*, 8–19. https://doi.org/10.1128/jvi.14.1.8-19.1974.

49. Honess, R.W., and Roizman, B. (1975). Regulation of herpesvirus macromolecular synthesis: sequential transition of polypeptide synthesis requires functional viral polypeptides. Proc. Natl. Acad. Sci. USA *72*, 1276–1280. https://doi.org/10.1073/pnas.72.4.1276.

50. Tombácz, D., Tóth, J.S., Petrovszki, P., and Boldogkoi, Z. (2009). Whole-genome analysis of pseudorabies virus gene expression by real-time quantitative RT-PCR assay. BMC Genom. *10*, 491. https://doi.org/10.1186/1471-2164-10-491.

51. Tombácz, D., Balázs, Z., Csabai, Z., Moldován, N., Szücs, A., Sharon, D., Snyder, M., and Boldogköi, Z. (2017). Characterization of the Dynamic Transcriptome of a Herpesvirus with Long-read Single Molecule Real-Time Sequencing. Sci. Rep. *7*, 1–13. https://doi.org/10.1038/srep43751.

52. Taddeo, B., Zhang, W., and Roizman, B. (2009). The virion-packaged endoribonuclease of herpes simplex virus 1 cleaves mRNA in polyribosomes. Proc. Natl. Acad. Sci. USA *106*, 12139–12144. https://doi.org/10.1073/pnas.0905828106.

53. Taddeo, B., Zhang, W., and Roizman, B. (2006). The UL41 protein of herpes simplex virus 1 degrades RNA by endonucleolytic cleavage in absence of other cellular or viral proteins. Proc. Natl. Acad. Sci. *103*, 2827–2832. https://doi.org/10.1073/pnas.0510712103.

54. Taddeo, B., and Roizman, B. (2006). The Virion Host Shutoff Protein (UL41) of Herpes Simplex Virus 1 Is an Endoribonuclease with a Substrate Specificity Similar to That of RNase A. J. Virol. *80*, 9341–9345. https://doi.org/10.1128/JVI.01008-06.

55. Hare, D., Collins, S., Cuddington, B., and Mossman, K. (2016). The Importance of Physiologically Relevant Cell Lines for Studying Virus–Host Interactions. Viruses *8*, 297. https://doi.org/10.3390/v8110297.

56. Gokhale, N.S., McIntyre, A.B.R., McFadden, M.J., Roder, A.E., Kennedy, E.M., Gandara, J.A., Hopcraft, S.E., Quicke, K.M., Vazquez, C., Willer, J., et al. (2016). N6-Methyladenosine in Flaviviridae Viral RNA Genomes Regulates Infection. Cell Host Microbe *20*, 654–665. https://doi.org/10.1016/j.chom.2016.09.015.

57. Tan, B., Liu, H., Zhang, S., Da Silva, S.R., Zhang, L., Meng, J., Cui, X., Yuan, H., Sorel, O., Zhang, S.W., et al. (2018). Viral and cellular N6-methyladenosine and N6,2′-O-dimethyladenosine epitranscriptomes in the KSHV life cycle. Nat. Microbiol. *3*, 108–120. https://doi.org/10.1038/s41564-017-0056-8.

58. Hesser, C.R., Karijolich, J., Dominissini, D., He, C., and Glaunsinger, B.A. (2018). N6-methyladenosine modification and the YTHDF2 reader protein play cell type specific roles in lytic viral gene expression during Kaposi's sarcoma-associated herpesvirus infection. PLoS Pathog. *14*, e10069955. https://doi.org/10.1371/journal.ppat.1006995.

59. Tirumuru, N., Zhao, B.S., Lu, W., Lu, Z., He, C., and Wu, L. (2016). N6-methyladenosine of HIV-1 RNA regulates viral infection and HIV-1 Gag protein expression. Elife *5*, e155288. https://doi.org/10.7554/eLife.15528.

60. Imam, H., Khan, M., Gokhale, N.S., McIntyre, A.B.R., Kim, G.-W., Jang, J.Y., Kim, S.-J., Mason, C.E., Horner, S.M., and Siddiqui, A. (2018). N6 -methyladenosine modification of hepatitis B virus RNA differentially regulates the viral life cycle. Proc. Natl. Acad. Sci. USA

115, 8829–8834. https://doi.org/10.1073/pnas.1808319115.

61. Williams, G.D., Gokhale, N.S., and Horner, S.M. (2019). Regulation of Viral Infection by the RNA Modification N6 -Methyladenosine. Annu. Rev. Virol. *6*, 235–253. https://doi.org/10.1146/annurev-virology-092818-015559.

62. Xue, M., Zhao, B.S., Zhang, Z., Lu, M., Harder, O., Chen, P., Lu, Z., Li, A., Ma, Y., Xu, Y., et al. (2019). Viral N6-methyladenosine upregulates replication and pathogenesis of human respiratory syncytial virus. Nat. Commun. *10*, 4595. https://doi.org/10.1038/s41467-019-12504-y.

63. Seyffert, M., Georgi, F., Tobler, K., Bourqui, L., Anfossi, M., Michaelsen, K., Vogt, B., Greber, U.F., and Fraefel, C. (2021). The HSV-1 Transcription Factor ICP4 Confers Liquid-Like Properties to Viral Replication Compartments. Int. J. Mol. Sci. *22*, 4447. https://doi.org/10.3390/ijms22094447.

64. Metrick, M.C., Loenigsberg, K.A., and Eeldwein, H.E. (2020). Conserved Outer Tegument Component UL11 from Herpes Simplex Virus 1 Is an Intrinsically Disordered, RNA-Binding Protein. mBio *11*, e00810–e00820. https://doi.org/10.1128/mBio.00810-20.

65. Shulman, Z., and Stern-Ginossar, N. (2020). The RNA modification N6-methyladenosine as a novel regulator of the immune system. Nat. Immunol. *21*, 501–512. https://doi.org/10.1038/s41590-020-0650-4.

66. Hesser, C.R., and Walsh, D. (2023). YTHDF2 Is Downregulated in Response to Host Shutoff Induced by DNA Virus Infection and Regulates Interferon-Stimulated Gene Expression. J. Virol. *97*, e0175822. https://doi.org/10.1128/jvi.01758-22.

67. Kretschmer, S., and Lee-Kirsch, M.A. (2017). Type I interferon-mediated autoinflammation and autoimmunity. Curr. Opin. Immunol. *49*, 96–102. https://doi.org/10.1016/j.coi.2017.09.003.

68. Bartkoski, M.J., and Roizman, B. (1978). Regulation of herpesvirus macromolecular synthesis VII. Inhibition of internal methylation of mRNA late in infection. Virology *85*, 146–156. https://doi.org/10.1016/0042-6822(78)90419-1.

69. Bartkoski, M., and Roizman, B. (1976). RNA synthesis in cells infected with herpes simple virus. XIII. Differences in the methylation patterns of viral RNA during the reproductive cycle. J. Virol. *20*, 583–588.

70. Srinivas, K.P., Depledge, D.P., Abebe, J.S., Rice, S.A., Mohr, I., and Wilson, A.C. (2021). Widespread remodeling of the m 6 A RNA-modification landscape by a viral regulator of RNA processing and export. Proc. Natl. Acad. Sci. USA *118*, e2104805118. https://doi.org/10.1073/pnas.2104805118.

71. Jansens, R.J.J., Verhamme, R., Mirza, A.H., Olarerin-George, A., Van Waesberghe, C., Jaffrey, S.R., and Favoreel, H.W. (2022). Alphaherpesvirus US3 protein-mediated inhibition of the m6A mRNA methyltransferase complex. Cell Rep. *40*, 111107. https://doi.org/10.1016/j.celrep.2022.111107.

72. Jansens, R.J.J., Marmiroli, S., and Favoreel, H.W. (2020). An Unbiased Approach to Mapping the Signaling Network of the Pseudorabies Virus US3 Protein. Pathogens *9*, 916. https://doi.org/10.3390/pathogens9110916.

73. Harkness, J.M., Kader, M., and DeLuca, N.A. (2014). Transcription of the Herpes Simplex Virus 1 Genome during Productive and Quiescent Infection of Neuronal and Nonneuronal Cells. J. Virol. *88*, 6847–6861. https://doi.org/10.1128/jvi.00516-14.

74. Romero, N., Wuerzberger-Davis, S.M., Van Waesberghe, C., Jansens, R.J., Tishchenko, A., Verhamme, R., Miyamoto, S., and Favoreel, H.W. (2022). Pseudorabies Virus Infection Results in a Broad Inhibition of Host Gene Transcription. J. Virol. *96*, e0071422. https://doi.org/10.1128/jvi.00714-22.

75. Nauwynck, H.J., and Pensaert, M.B. (1995). Effect of specific antibodies on the cell-associated spread of pseudorabies virus in monolayers of different cell types. Arch. Virol. *140*, 1137–1146. https://doi.org/10.1007/BF01315422.

76. Olsen, L.M., Ch'ng, T.H., Card, J.P., and Enquist, L.W. (2006). Role of pseudorabies virus Us3 protein kinase during neuronal infection. J. Virol. *80*, 6387–6398. https://doi.org/10.1128/JVI.00352-06.

77. de Wind, N., Zijderveld, A., Glazenburg, K., Gielkens, A., and Berns, A. (1990). Linker insertion mutagenesis of herpesviruses: inactivation of single genes within the Us region of pseudorabies virus. J. Virol. *64*, 4691–4696.

78. SMITH, K.O. (1964). RELATIONSHIP BETWEEN THE ENVELOPE AND THE INFECTIVITY OF HERPES SIMPLEX VIRUS. Proc. Soc. Exp. Biol. Med. *115*, 814–816. https://doi.org/10.3181/00379727-115-29045.

79. Read, G.S., Karr, B.M., and Knight, K. (1993). Isolation of a herpes simplex virus type 1 mutant with a deletion in the virion host shutoff gene and identification of multiple forms of the vhs (UL41) polypeptide. J. Virol. *67*, 7149–7160. https://doi.org/10.1128/JVI.67.12.7149-7160.1993.

80. Ejercito, P.M., Kieff, E.D., and Roizman, B. (1968). Characterization of herpes simplex virus strains differing in their effects on social behaviour of infected cells. J. Gen. Virol. *2*, 357–364. https://doi.org/10.1099/0022-1317-2-3-357.

81. Dobin, A., Davis, C.A., Schlesinger, F., Drenkow, J., Zaleski, C., Jha, S., Batut, P., Chaisson, M., and Gingeras, T.R. (2013). STAR: Ultrafast universal RNA-seq aligner. Bioinformatics *29*, 15–21. https://doi.org/10.1093/bioinformatics/bts635.

82. Love, M.I., Huber, W., and Anders, S. (2014). Moderated estimation of fold change and dispersion for RNA-seq data with DESeq2. Genome Biol. *15*, 550–621. https://doi.org/10.1186/s13059-014-0550-8.

83. Geenen, K., Favoreel, H.W., and Nauwynck, H.J. (2005). Higher resistance of porcine trigeminal ganglion neurons towards pseudorabies virus-induced cell death compared with other porcine cell types in vitro. J. Gen. Virol. *86*, 1251–1260. https://doi.org/10.1099/vir.0.80760-0.

84. Schwartz, S., Mumbach, M.R., Jovanovic, M., Wang, T., Maciag, K., Bushkin, G.G., Mertins, P., Ter-Ovanesyan, D., Habib, N., Cacchiarelli, D., et al. (2014). Perturbation of m6A writers reveals two distinct classes of mRNA methylation at internal and 5′ sites. Cell Rep. *8*, 284–296. https://doi.org/10.1016/j.celrep.2014.05.048.

85. He, S., Wang, H., Liu, R., He, M., Che, T., Jin, L., Deng, L., Tian, S., Li, Y., Lu, H., et al. (2017). mRNA N6-methyladenosine methylation of postnatal liver development in pig. PLoS One *12*, e01734211. https://doi.org/10.1371/journal.pone.0173421.

86. Wang, Y., Li, Y., Toth, J.I., Petroski, M.D., Zhang, Z., and Zhao, J.C. (2014). N6-methyladenosine modification destabilizes developmental regulators in embryonic stem cells. Nat. Cell Biol. *16*, 191–198. https://doi.org/10.1038/ncb2902.

87. Gaidatzis, D., Lerch, A., Hahne, F., and Stadler, M.B. (2015). QuasR: Quantification and annotation of short reads in R. Bioinformatics *31*, 1130–1132. https://doi.org/10.1093/bioinformatics/btu781.

88. Romero, N., Van Waesberghe, C., and Favoreel, H.W. (2020). Pseudorabies Virus Infection of Epithelial Cells Leads to Persistent but Aberrant Activation of the NF-κB Pathway, Inhibiting Hallmark NF-κB-Induced Proinflammatory Gene Expression. J. Virol. *94*, e00196-20. https://doi.org/10.1128/JVI.00196-20.

89. Piret, J., Roy, S., Gagnon, M., Landry, S., Désormeaux, A., Omar, R.F., and Bergeron, M.G. (2002). Comparative study of mechanisms of herpes simplex virus inactivation by sodium lauryl sulfate and n-lauroylsarcosine. Antimicrob. Agents Chemother. *46*, 2933–2942. https://doi.org/10.1128/AAC.46.9.2933-2942.2002.

STAR★METHODS

KEY RESOURCES TABLE

REAGENT or RESOURCE	SOURCE	IDENTIFIER
Antibodies		
PRV gE	Nauwynck and Pensaert[75]	N/A
PRV US3	Olsen et al.[76]	N/A
YTHDF1	Proteintech	17479-1-AP; RRID: AB_2217473
YTHDF2	Proteintech	24744-1-AP; RRID: AB_2687435
YTHDF3	Proteintech	25537-1-AP; RRID: AB_2847817
YTHDC1	Abcam	ab122340; RRID: AB_11128253
YTHDC2	Proteintech	27779-1-AP; RRID: AB_2880970
CNOT1	Proteintech	14276-1-AP; RRID: AB_10888627
EDC4	Santa Cruz Biotechnology	sc-376382; RRID: AB_10988077
Alpha-tubulin	Abcam	ab40742; RRID: AB_880625
Anti-mouse HRP Secondary	Agilent	P0447; RRID: AB_2617137
Anti-rabbit HRP Secondary	Agilent	P0448; RRID: AB_2617138
Bacterial and virus strains		
PRV NIA3 WT	de Wind et al.[77]	N/A
PRV NIA3 UL41null	de Wind et al.[77]	N/A
HSV1 Kos WT	Smith[78]	N/A
HSV1 Kos vhsnull	Read et al.[79]	N/A
HSV1 F WT	Ejercito et al.[80]	N/A
Chemicals, peptides, and recombinant proteins		
MEM	Gibco	41090–028
DMEM	Gibco	61965–026
PhosStop	Roche	4906845001
PVDF membrane	Amersham	10600023
Phosphonoacetic acid	Sigma-Aldrich	284270
RIPA buffer	Abcam	ab156034
cOmplete mini EDTA free protease inhibitor	Roche	11836170001
Hoechst 33342, Trihydrochloride, Trihydrate	Thermo Fisher Scientific	H1399
Nonidet P-40 lysis buffer	Merck	11332473001
Pierce enhanced chemiluminescence (ECL) substrate	Thermo Scientific	32106
ECL Plus substrate	GE Healthcare	RPN2236
SuperSignal West Femto maximum sensitivity substrate	Thermo Scientific	54095
Critical commercial assays		
SYBR Green PCR Master Mix	Applied Biosystems	4309155
RNeasy Mini Kit	Qiagen	74106
iScript cDNA Synthesis Kit	Bio-Rad	1708891
QuantSeq 3′ mRNA library prep FWD kit	Lexogen	
On-column RNase-Free DNase Set	Qiagen	79254

(*Continued on next page*)

Continued

REAGENT or RESOURCE	SOURCE	IDENTIFIER
Deposited data		
Previously published RNA-seq data	Table S1	Table S1
M6A map pig liver cells	N/A	GEO: GSE87327
M6A map HEK293T cells	Linder et al.[36]	N/A
Generated raw RNA-seq data	This paper	GEO: GSE201012
Generated code	This paper	Zenodo: https://doi.org/10.5281/zenodo.8085292
Experimental models: Cell lines		
ST cells	ATCC	RRID:CVCL_2204
HEK293T cells	ATCC	RRID:CVCL_0063
HeLa cells	ATCC	RRID:CVCL_0030
Oligonucleotides		
siRNA oligonucleotides		N/A
Scrambled Negative Control DsiRNA	IDT	51-01-19-09
Oligonucleotides for RT-qPCR		N/A
Software and algorithms		
GraphPad Prism	GraphPad Software Inc	https://www.graphpad.com/
RStudio 2021.09.2	RStudio	www.rstudio.com
R-4.1.2	R project	https://www.r-project.org/
STAR 2.7.4a	Dobin et al.[81]	https://github.com/alexdobin/STAR
DESeq2	Love et al.[82]	https://bioconductor.org/packages/release/bioc/html/DESeq2.html
ImageJ	NIH Image for the Macintosh	https://imagej.nih.gov/ij/
Leica LAS X confocal microscopy software	Leica Microsystems	https://www.leica-microsystems.com/products/microscope-software/p/leica-las-x-ls/
Other		
NextSeq 500 SR 76 high output system	Illumina	N/A
Quant-it Ribogreen RNA assay	Life Technologies	N/A
RNA 6000 nano chip	Agilent Technologies	N/A

RESOURCE AVAILABILITY

Lead contact

Further information and requests for resources and reagents should be directed to and will be fulfilled by the Lead Contact, Herman Favoreel (herman.favoreel@ugent.be).

Materials availability

This study did not generate new unique reagents.

Data and code availability

- The RNA-seq data reported in this paper have been deposited at Gene Expression Omnibus (GEO) and are publicly available. Accession numbers are listed in the key resources table.
- All original code has been deposited at Zenodo and is publicly available. DOIs are listed in the key resources table.
- Any additional information required to reanalyze the data reported in this paper is available from the lead contact upon request.

EXPERIMENTAL MODEL AND STUDY PARTICIPANT DETAILS

Cells and viruses

Swine testicle (ST) cells were cultured in MEM (Gibco) supplemented with 10% fetal calf serum (FCS), 1 mM sodium pyruvate, 105 U/l penicillin, 100 mg/L streptomycin and 50 mg/L gentamycin. Confluent cells were infected at a MOI 10 and lysed at 16 hpi. HEK293T and HeLa cells were cultured in DMEM (Gibco) supplemented with 10% FCS, 10^5 U/l penicillin, 100 mg/L streptomycin and 50 mg/L gentamycin. Primary porcine kidney (PPK) cells were isolated as described previously,[83] and were cultured in MEM (Gibco) supplemented with 10% FCS, 105 U/l penicillin and 50 mg/L gentamycin. Cells were kept at 37°C in a humidified atmosphere at 5% CO_2.

Wild type HSV-1 F strain was described previously,[80] as well as wild type HSV-1 KOS strain and vhsnull strain.[78,79] Wild type and UL41null NIA3 was previously described and was kindly donated by the ID-DLO (The Netherlands).[77]

METHOD DETAILS

Sequencing and analysis

RNA isolations were performed using the RNeasy mini kit (Qiagen) according to the manufacturer's procedure. Dnase treatment was performed on-column to eliminate DNA contamination (79254, Qiagen). Concentration and quality of the total extracted RNA was checked via the Quant-it Ribogreen RNA assay (Life Technologies) and the RNA 6000 nano chip (Agilent Technologies). The QuantSeq 3′ mRNA library prep FWD kit (Lexogen) was used for library preparation. Library QC was performed using the high sensitivity DNA chip (Agilent technologies). Sequencing was performed on the NextSeq 500 SR 76 high output system (Illumina). All sequencing data was deposited under the following accession number in GEO: GSE201012.

To determine the difference in gene expression of m6A-methylated transcripts compared to unmethylated transcripts, differential expression was determined for transcripts binned by the amount of m6A residues they contain. Previously published RNA-seq datasets comparing uninfected and virus-infected cells were used for these analyses, with RNA-seq performed at the indicated time points after infection (Table S1). Reads were aligned to the Sscrofa11.1, mm39 or hg38 genomes using STAR.[81] Differential expression was determined using DESeq2.[82] Methylation of transcripts is generally highly similar in different cell lines,[84] so previously described m6A mapping data could be used to estimate the number of m6A sites per mRNA in a cell line/tissue of interest for which there is no m6A map. For porcine samples, we used an m6A map from pig liver cells (GEO: GSE87327).[85] For the murine dataset an m6A map based on mESCs was used.[86] For the analyses of human samples, an m6A map originating from HEK293T cells was used.[36] Tables S2, S3, and S4 contain overviews of the number of m6A methylation sites of each transcripts in these m6A maps. Graphs of the cumulative fold change between two conditions were generated by binning transcripts by the amount of m6A residues.

To differentiate between alterations in transcript stability and changes in transcription rates, exon-intron split analysis (EISA) was performed. EISA measures changes in mature mRNA (which lack introns) and pre-mRNA (which contain introns) to quantify transcriptional and post-transcriptional regulation of gene expression.[46] This approach results in a measure for changes in transcription rate (Δintron) and a measure for changes in transcript stability (Δexon – Δintron) for each transcript. Sequencing reads were aligned using the quasr package in R.[87] Exonic and intronic reads were counted based on the Sscrofa11.1 reference genome using qcount. Δintron and Δexon were determined using the eisaR package in R.[46]

M6A reader knockdown

YTH readers were knocked down in ST cells using the DsiRNA system from IDT. siRNAs targeting porcine readers were designed using the design tool from IDT (Table S5). siRNAs were transfected using lipofectamine RNAiMAX (ThermoFisher) according to the manufacturer's instructions. In brief, 2.5 μL of a 10 μM stock of siRNA and 7.5 μL of lipofectamine RNAiMAX were used for a well of a six well plate. All experiments were performed using Scrambled Negative Control DsiRNA as a negative control (51-01-19-09, IDT). At 48 hpt, knockdown cells were infected and processed further.

Cell treatments

Phosphonoacetic acid (PAA) was obtained from Sigma-Aldrich (catalog no. 284270). Cells were treated with 400 μg/mL PAA starting from 30 min before virus inoculation and during the entire infection time, as described before.[88]

Immunofluorescence

Cells were fixed using 3% paraformaldehyde for 10 min after which they were permeabilized using 0.1% Triton X- for 10 min. Primary antibodies were incubated overnight at 4°C. Following 3 washing steps with PBS, cells were incubated with secondary antibody for 1 h at 37 °C at a 1/200 dilution. After three more washing steps with PBS, cells were mounted using glycerine-DABCO.

Stained samples were imaged using a Leica SPE laser scanning confocal microscope (Leica) or a Dmi8 Thunder inverted microscope (Leica). Images were processed and analyzed using FIJI. For the quantification of P-bodies the analyze particles function was used, with a minimum size of 10 pixels, after setting a threshold of 150 to determine EDC4 puncta. Colocalization of YTHDF proteins and P-bodies was quantified by measuring the degree of overlap of the fluorescence signal in the YTHDF channel with the fluorescence signal in the EDC4 channel using Fiji. Per condition, for each of the three independent replicate samples, three random fluorescence images taken with a Leica Dmi8 Thunder inverted microscope (Leica) were used for analysis. Immunofluorescence assays were performed using primary antibodies against YTHDF1 (Proteintech 17479-1-AP, 1/100), YTHDF3 (Proteintech 25537-1-AP, 1/100 and EDC4 (Santa Cruz Biotechnology sc-376382, 1/100).

Western blotting

Cells were lysed at 16 hpi in RIPA buffer (Abcam) with cOmplete mini EDTA free protease inhibitor cocktail (Roche) and PhosStop (Roche). Cell lysates were separated on a 10% polyacrylamide gel, followed by blotting on PVDF membrane (Amersham). Blots were blocked in 5% nonfat milk diluted in 0.1% Tween 20 in PBS for 1 h at room temperature. Primary antibodies were incubated overnight at 4°C. Following 3 consecutive 5 min washes in 0.1% Tween 20 in PBS, the membranes were incubated with the secondary antibody for 1 h at room temperature. Following 3 more 5 min washes, the blots were imaged using Pierce enhanced chemiluminescence (ECL) substrate (Thermo Scientific), ECL Plus substrate (GE Healthcare), or SuperSignal West Femto maximum sensitivity substrate (Thermo Scientific) on a ChemiDoc MP imaging device (Bio-Rad). Western blot assays were performed using primary antibodies against alpha-tubulin (Abcam ab40742, 1/1,000), YTHDF1 (Proteintech 17479-1-AP, 1/1,000), YTHDF2 (Proteintech 24744-1-AP, 1/1,000), YTHDF3 (Proteintech 25537-1-AP, 1/1,000), YTHDC1 (Abcam ab122340, 1/250), YTHDC2 (Proteintech 27779-1-AP, 1/500), CNOT1 (Proteintech 14276-1-AP, 1/1,000), PRV US3 (Leigh Anne Olsen and Lynn Enquist Princeton University, USA,[76] 1/100) and PRV gE (Hans Nauwynck Ghent University, Belgium,[75] 1/100).

Virus titrations

Confluent ST cell monolayers were infected at an MOI of 10 for 24 h and 48 h. Virus inoculum was washed away at 2 hpi, and the cells were washed twice with PBS. The cells were treated with sodium citrate buffer, pH 3.0 (40 mM sodium citrate, 10 mM KCl, 135 mM NaCl), for 2 min at room temperature to remove all remaining infectious virus from the input.[89] Following two more washing steps with PBS, fresh ST medium was added.

Infectious virus in the supernatants was titrated by 1/10 serial dilution assays on ST cells and four experimental repeats were performed. The characteristic PRV-derived cytopathic effect served as a readout. Titers are expressed as the log10 of the $TCID_{50}$/mL.

RNA isolation and real time quantitative PCR (RT-qPCR)

Total RNA isolations were performed using the Rneasy minikit (Qiagen) according to the manufacturer's instructions. Purified RNA was treated with on-column Rnase free Dnase (Qiagen) to remove contaminating DNA. Reverse transcription was carried out with 500 ng RNA using an iScript cDNA synthesis kit (Bio-Rad) according to the manufacturer's instructions. Quantitative PCR was performed using a StepOnePlus real-time PCR system (Applied Biosystems, Thermo Fisher Scientific) with SYBR green master mix (Applied Biosystems). The relative expression of each gene was analyzed by the double delta threshold cycle method and normalized to the level of expression of the 28S rRNA gene, which has been validated as a reference gene as previously described.[88] Primers used for the different genes are listed in Table S6.

Graphic illustrations

The graphic illustrations displayed in this paper were created with BioRender.com

QUANTIFICATION AND STATISTICAL ANALYSIS

For the statistical analysis of the results, either a Wilcoxon rank-sum test was used, or a two-sided unpaired t-test after confirmation of normality by Shapiro-Wilk test. P-values <0.05 were considered to be significant. Analysis and visualization were performed in R using ggplot2, except for Figures 5B, 5C, S2B, and S2C which were generated in Graphpad Prism.